Combustion of Renewable Biogas Fuels

Chaouki Ghenai[1] and Isam Janajreh[2]

1. *Sustainable and Renewable Energy Department, College of Engineering, University of Sharjah, Sharjah 27272, United Arab Emirates*

2. *Mechanical Engineering Program, MASDAR Institute of Science and Technology, Abu Dhabi 54224, United Arab Emirates*

Abstract: Biogas fuel is a sustainable and renewable fuel produced from anaerobic digestion of organic matter. The biogas fuel is a flammable mixture of methane and carbon dioxide with low to medium calorific values. Biogas is an alternative to conventional fossil fuels and can be used for heating, transportation and power generation. CFD (computational fluid dynamic) analysis of the combustion performance and emissions of biogas fuel in gas turbine engines is presented in this study. The main objective of this study is to understand the impact of the variability in the biogas fuel compositions and lower heating values on the combustion process. Natural gas, biogas from anaerobic digester, landfill biogas, and natural gas/biogas mixture fuels combustion were investigated in this study. The CFD results show lower peak flame temperature and CO mole fractions inside the combustor and lower NO_x emissions at the combustor exit for the biogas compared to natural gas fuel. The peak flame temperature decreases by 37% for the biogas landfill ($CO_2/CH_4 = 0.89$) and by 22% for the biogas anaerobic digester ($CO_2/CH_4 = 0.54$) compared to natural gas fuel combustion. The peak CO mole fraction inside the combustor decreases from 9.8×10^{-2} for natural gas fuel to 2.22×10^{-4} for biogas anaerobic digester and 1.32×10^{-7} for biogas landfill. The average NO_x mole fraction at the combustor exit decreases from 1.13×10^{-5} for natural gas fuel to 0.40×10^{-6} for biogas anaerobic digester and 1.06×10^{-10} for biogas landfill. The presence of non-combustible constituents in the biogas reduces the temperature of the flame and consequently the NO_x emissions.

Key words: Anaerobic digestion, biogas, non-premixed combustion, NO_x emissions, CFD.

1. Introduction

Most of the present energy demands (80%-85%) are provided through the combustion of fossil fuels (natural gas, oil and coal). The reliance on fossil fuels will diminish in the coming decades due to the new emissions regulations (reduction of carbon dioxides CO_2, other greenhouses gases such as NO_x and SO_x and particulate matter), depletion of fossil fuels (reduction of oil, natural gas and coal reserves), and the need of more renewable and sustainable energy systems [1]. Renewable power systems using renewable resources such as solar, wind, hydro, ocean, geothermal and biomass natural resources are alternatives to conventional power generation using coal, natural gas and oil fossil fuels [1]. Sustainable and renewable biofuels such as syngas, biogas, biodiesel, bioethanol and bio-oil are alternatives to conventional fuels that can be used for transportation, heating and power generation. Biofuels produced from biomass (sustainable energy sources: wood, plants, vegetable oils, green waste, animal waste and sludge) through thermal and biochemical conversion processes are good fuel candidates for the replacement of fossil fuels usage. The biofuels are more sustainable fuels produced from local and renewable resources and offer lower emissions compared to fossil fuels combustion.

Natural gas is used as the primary fuel in gas turbine engine combustors for power generation. The development and use of new renewable and alternative gas fuels such as biogas derived from anaerobic digester and landfills and syngas derived from biomass, coal and solid waste gasification processes present certain challenges that must be addressed. The alternative fuels such as syngas and biogas have different chemical compositions and heating values

Corresponding author: Chaouki Ghenai, assistant professor, research fields: renewable energy, energy efficiency, alternative fuels, combustion and sustainability. E-mail: cghenai@sharjah.ac.ae.

compared to natural gas fuels. The lower heating values (MJ/kg) of alternatives fuels such as syngas and biogas are much lower than heating value of natural gas. For the same combustor power, the fuel mass flow for syngas and biogas should be much greater than for natural gas, due to the lower heating values. Lean turbulent premixed combustions are usually used for gas turbine engines to control the NO_x emissions [2]. The combustion systems using lean combustion technologies cannot be used for syngas fuels with high hydrogen (60%-70%) content due to the potential for flashback of the flame into the fuel injection systems. Non-premixed combustors are more appropriate for synags fuels with high hydrogen contents [2]. The flame temperature and NO_x emissions can be controlled by diluting the syngas fuels with inert gas. Natural gas is made mainly of methane (CH_4), syngas fuel contains methane (CH_4), carbon dioxide (CO_2), carbon monoxide (CO), hydrogen (H_2), nitrogen (N_2) and water (H_2O), and biogas contains mainly methane (CH_4) and carbon dioxide (CO_2). The changes in the fuel compositions and lower heating values for alternative gas fuels (syngas and biogas) affect the combustion process, the efficiency of the combustion system and the gas emissions at the exit from the combustor [3]. The new gas turbine combustors for renewable and biofuels should be able to burn a wide variety of gases (syngas, biogas and other alternative gas fuels) with low, medium and high heating values. The new combustors should be able to handle syngas fuels with high hydrogen content (high flame speed and flame stability problems). The new alternative fuels (biogas and syngas) must be burned efficiently in the combustors. The NO_x and CO_2 emissions from the combustion of syngas and biogas fuels should be comparable or better than those obtained with natural gas fuels. Better understanding of the physical and chemical processes of syngas and biogas combustion is needed in order to meet these challenges and help the development and use of biofuels in existing or new combustion systems.

Information such as flame shape, flame speed, turbulent flow/flame interactions, gas temperatures and pollutant emissions (NO_x and CO_2) for a range of alternative fuels compositions and heating values is needed for the design of gas turbine combustors.

The syngas produced from renewable energy sources will help to reduce emissions from combustion systems and increase the energy security (offsets non-renewable resources—coal, oil, natural gas). Brdar and Jones [4] investigated the integration of heavy-duty gas turbine technology with synthetic fuel gas processes. They summarized in this study the experience gained from several syngas projects and lessons learned with respect to cost reductions and improving the operational reliability of gas turbine. They concluded that, further improvements are needed for syngas use in gas turbine engines especially with respect to system performance and plant design. The results of the combustion of low calorific syngas fuels derived from gasification of waste biomass were presented by Kwiatkowski, et al. [5]. Computational fluid dynamics of the combustion of two different gases derived from gasification of waste wood chips and turkeys feathers was presented in this paper. The result shows that, low calorific syngas from waste biomass including gas derived from the gasification of feathers can be valuable fuel for direct combustion on industrial scale. The impact of firing syngas in gas turbine engines was investigated experimentally by Oluyede [6]. The results of the experimental investigation show that, volume fraction of hydrogen content in syngas fuel results in higher flame temperature that significantly impacts the life of hot sections of the combustor. Giles, et al. [7], Ghenai [3] and Zbeeb and Ghenai [8] performed numerical investigations on the effects of syngas compositions and diluents on the flame structure and emissions for non-premixed combustion. For premixed combustion, lean premixed combustion of hydrogen-syngas/methane fuel mixtures was investigated experimentally by Alavandi and Agarwal [9]

and Schefer [10]. In their studies, they investigated the effect of hydrogen content in syngas fuels on the biofuels combustion process. Rahm, et al. [11] addressed the challenges of fuel diversity use and the corresponding environmental and engine performance impacts. They reviewed the combustion design flexibility for the use of a different gas and liquid fuels including emerging synthetic fuels. The synthetic gases included low heating value process gas, syngas, ultra-high hydrogen or higher heating values fuels.

In anaerobic digester process, micro-organisms break down biodegradable material in the absence of oxygen to produce biogas and digester by products as shown in Fig. 1. The biogas feed stocks or digester inputs include organic matter from plants and animals, waste water, and food processing waste. The biogas produced can be burned and used for different applications (Fig. 1). Biogas can be used to offset non-renewable resources; biogas is produced using renewable energy resources; and offer environmental benefits by reducing the emissions by preventing CH_4 release to the atmosphere and reducing landfill wastes and odors. Razbani, et al. [12] performed a literature review on biogas use in internal combustion engines. He reviewed the challenges such as lower flame speed compared to natural gas, biogas impurities, and combustion characteristics of biogas fuel in reciprocating engines. Solutions such as advanced spark timing, increasing compression ratio, changing bearing and piston materials were presented. Laminar burning velocities of biogas-air mixtures in premixed combustion have been studied to elucidate the fundamental flame propagation characteristic of biogas as a new alternative and renewable fuel [13] in spark ignition engine. The results show that, the laminar burning velocities of biogas-air mixtures were lower than those in methane-air mixtures at the same equivalence ratio because biogas contains carbon dioxide and nitrogen which are flame inhibitors. Barik, et al. [14] reviewed the current status and perspectives of biogas production, including the storage methods

and its engine application. The study concluded the potential of biogas production from various organic biomass wastes. Attention was also focused for making biogas as a transport vehicle and stationary engine fuel by storing it in cylinders and reinforced plastic bags. Colorado, et al. [15] investigated the performance of flameless combustion using biogas and natural gas fuels. The results show minor reduction of the efficiency of the furnace and lower temperatures for the biogas fuels.

This study focuses on the combustion performance and emissions of biogas fuels. The design of new combustion systems using sustainable and alternative fuels such as biogas fuel can take advantage of computational fluid dynamics analysis to optimize the efficiency of the combustion process and to reduce the pollutants emission. The principal objective of this study is to analyze the fundamental impacts of firing biogas in gas turbine combustor and predict the changes in the firing temperature and emissions with respect to natural gas combustion.

2. Governing Equations—Natural Gas and Biogas Combustion Modeling

The equations used for natural gas, biogas, and natural gas/biogas mixture fuels combustion modeling [3] are based on the equations of conservation of mass, momentum and energy, the equations of the turbulent kinetic energy k and the dissipation rate of the turbulent kinetic energy the ε standard k-ε turbulence model), the mixture fraction equation (mixture fraction/PDF (probability density function)) model for non-premixed combustion modeling), and the equation to simulate the radiation from the flame (P-1 radiation model). For steady turbulent non premixed combustion [3], the time averaged gas phase equations are summarized in Table 1. It is noted that, ρ is the density, u is the velocity, P is the pressure, τ is the shear stress, k is the turbulent kinetic energy, ε is the dissipation of the turbulent kinetic energy and μ is the dynamic viscosity. For the turbulent kinetic energy

and dissipation of the kinetic energy equations, $\sigma_k = 1$, G_k is the production of the turbulent kinetic energy and $C_{\varepsilon 1} = 1.44$, $C_{\varepsilon 2} = 1.92$ and $\sigma_\varepsilon = 1.3$. For the mixture fraction equation and non-premixed (diffusion flame) combustion, the PDF/mixture fraction model is used in this study. First, the equation for the mixture fraction f is solved, and individual component concentrations are derived from the predicted mixture
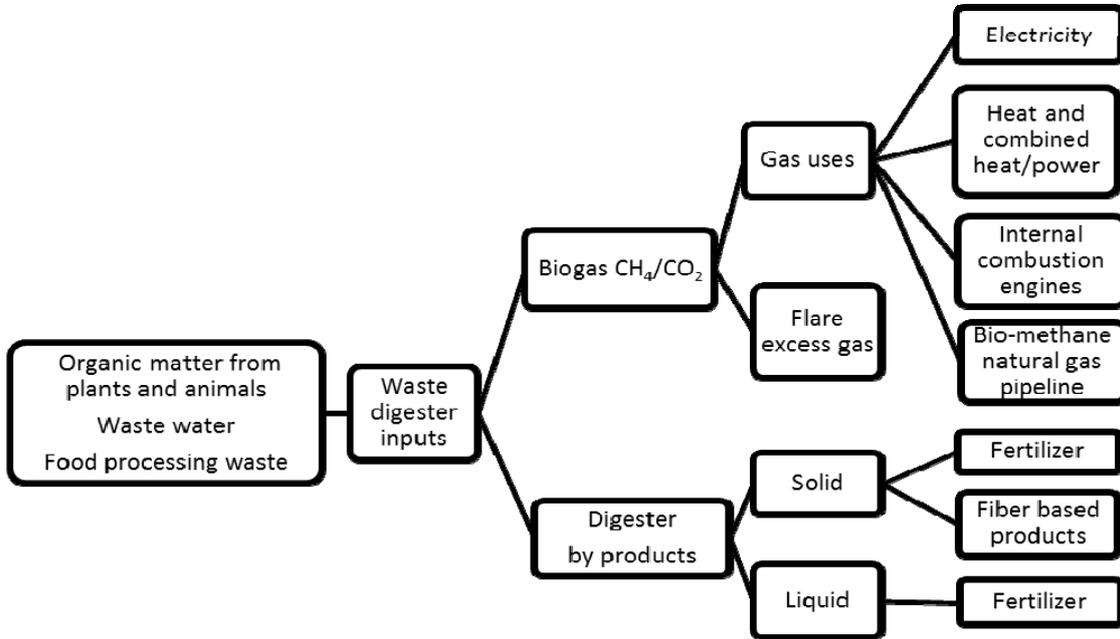

Fig. 1   Biogas production and utilization.

Table 1   Governing equations.

	Equations
Continuity	$\dfrac{\partial \overline{\rho\, u_i}}{\partial x_i} = 0$
Momentum	$\dfrac{\partial\left(\overline{\rho u_i u_j}\right)}{\partial x_j} = -\dfrac{\partial \overline{P}}{\partial x_i} + \dfrac{\partial\left(\overline{t_{ij}} + \overline{\tau_{ij}}\right)}{\partial x_j}$
Turbulent kinetic energy	$\dfrac{\partial\left(\overline{\rho\, k\, u_j}\right)}{\partial x_j} = \dfrac{\partial\left[\left(\mu + \dfrac{\mu_t}{\sigma_k}\right)\dfrac{\partial \overline{k}}{\partial x_j}\right]}{\partial x_j} + G_k - \overline{\rho\, \varepsilon}$
Dissipation of the kinetic energy	$\dfrac{\partial\left(\overline{\rho\, \varepsilon\, u_j}\right)}{\partial x_j} = C_{\varepsilon 1}\dfrac{\overline{\varepsilon}}{k} G_k + \dfrac{\partial\left[\left(\mu + \dfrac{\mu_t}{\sigma_\varepsilon}\right)\dfrac{\partial \overline{\varepsilon}}{\partial x_j}\right]}{\partial x_j} - C_{\varepsilon 2}\overline{\rho}\dfrac{\overline{\varepsilon^2}}{k}$
Mixture fraction f	$\dfrac{\partial\left(\overline{\rho\, f\, u_j}\right)}{\partial x_j} = \dfrac{\partial\left[\left(\dfrac{\mu_t}{\sigma_t}\right)\dfrac{\partial \overline{f}}{\partial x_j}\right]}{\partial x_j} + S_m$
Energy	$\dfrac{\partial\left(\overline{\left(\rho\, E + p\right)uj}\right)}{\partial x_j} = \dfrac{\partial\left[\left(k_{eff}\right)\dfrac{\partial \overline{T}}{\partial x_j} - \sum_j h_j J_j + \left(\overline{\tau}_{eff} u_j\right)\right]}{\partial x_j} + S_h$
Radiation	$q_r = -\dfrac{1}{3\left(a + \sigma_S\right) - C\sigma_S}\nabla G$

fraction distribution [3]. The mixture fraction f is given by $f = (Z_k - Z_{k,O})/(Z_{k,F} - Z_{k,O})$, where Z_k is the element mass fraction of element k. Subscripts F and O denote fuel and oxidizer inlet stream values, respectively. The chemistry is assumed to be fast enough to achieve equilibrium. The equilibrium chemistry PDF model was used and 13 species (C, CH_4, CO, CO_2, H, H_2, H_2O, N_2, NO, O, O_2, OH, HO_2) were selected for the combustion modeling. In the energy equation (Table 1), E is the total energy ($E = h - p/\rho + v^2/2$, where h is the sensible enthalpy), k_{eff} is the effective conductivity ($k + k_t$: laminar and turbulent thermal conductivity), J_j is the diffusion flux of species j, and S_h is the term source that includes the heat of chemical reaction, radiation and any other volumetric heat sources. The P-1 radiation model was used in this study to simulate the radiation from the flame [3]. This model is based on the expansion of the radiation intensity into an orthogonal series of spherical harmonics (Cheng [16] and Siegel and Howell [17]). The P-1 radiation model is the simplest case of the P-N model [3]. If only four terms in the series are used, the equation q_r for the radiation flux is obtained (Table 1), where, a is the absorption coefficient, σ_S is the scattering coefficient, G is the incident radiation and C is the linear-anisotropic phase function coefficient (Cheng [16] and Siegel and Howell [17]).

For NO_x modeling, the nitrogen oxides concentrations emitted from combustion systems are generally low, the NO_x chemistry has negligible influence on the predicted temperature, velocity field, and species concentrations. First, the main combustion calculations were performed then the NO_x emissions were calculated using the NO_x model (post-processing calculations). The reacting flows are simulated without NO_x emissions first until the convergence of the main combustion calculation was obtained, then the desired NO_x models (thermal and prompt NO_x) were enabled to predict the NO_x emissions.

For the numerical method, the finite volume and the first order upwind methods are used in this study to solve the governing equations. The solution procedure for mixture-fraction system is to complete first the calculation of the PDF look-up tables, start the reacting flow simulation to determine the flow files and predict the spatial distribution of the mixture fraction, continue the reacting flow simulation until a convergence solution was achieved, and determine the corresponding values of the temperature and individual chemical species mass fractions from the look-up tables. The convergence criteria for the continuity, momentum, turbulent kinetic energy, dissipation rate of the turbulent kinetic energy, and the mixture fraction were set to 10^{-3}. For the energy and the radiation equations, the convergence criteria were set to 10^{-6}.

3. Combustor Geometry Model and Composition and Lower Heating Values of Fuels

Fig. 2 shows the gas turbine can combustor geometry model used for this study. The combustor is similar to the one used by Ghenai [3] for the simulation of syngas fuels. The dimension of the can combustor is 590 mm in the z direction (longitudinal direction), 250 mm in the y direction and 230 mm in the x direction [3]. The primary air injected inside the can combustor is guided by air vanes to give swirling (Fig. 2). The primary air is injected from a an injection diameter of 85 mm with a velocity of 10 m/s, a temperature of 300 K (or 27 °C), turbulence intensity of 10%, and with zero mixture fraction ($f = 0$). The natural gas and biogas fuels are injected through six fuel injectors in the swirling primary air flow as shown in Fig. 2. It is noted that, the fuel mass flow rate (Table 2) was varied to keep the same power or rate of heat flow (watts or J/s) for the five fuels tested in this study. The fuel is injected through an injection diameter of 4.2 mm with a temperature of 300 K, a turbulence intensity of 10%, and a mixture fraction

(a)

(b)

(c)
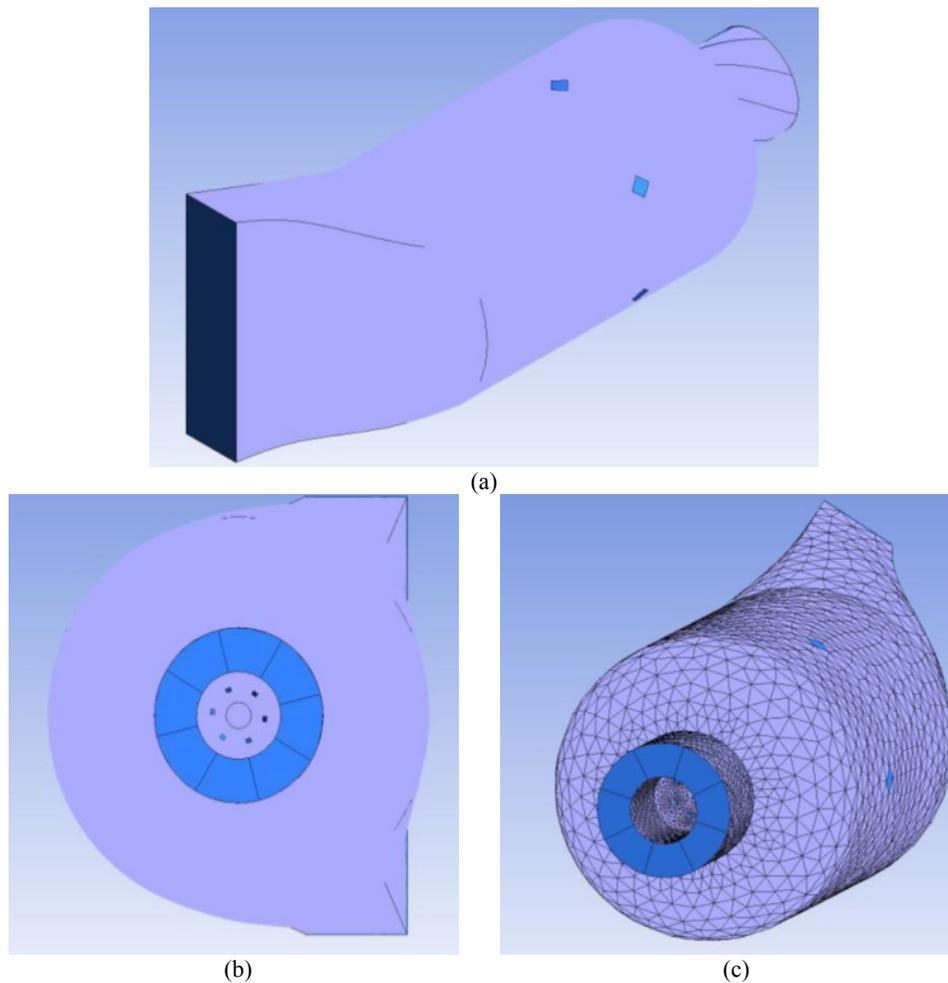
Fig. 2   Swirl can combustor geometry and mesh.

Table 2   Fuel composition—natural gas and low and high grade biogas.

	NG	Mixture 50% NG 50% BGAD	Mixture 50% NG 50% BGLF	Biogas anaerobic digester BGAD	Biogas landfill BGLF
CH$_4$ (%)	95	80	70	65	45
CO$_2$ (%)	0	17.5	20	35	40
N$_2$ (%)	2	1	8.5	0	15
C$_2$H$_6$ (%)	3	1.5	1.5	0	0
LHV (MJ/kg)	50	35	31	20	12.3
Fuel mass flow rate (kg/s)	1.0×10^{-3}	1.4×10^{-3}	1.6×10^{-3}	2.5×10^{-3}	4.06×10^{-3}
Power (kW)	50	50	50	50	50

NG: natural gas; BGAD: biogas anaerobic digester; BGAD: biogas landfill; LHV: lower heating values.

$f = 1$. To control the flame temperature and NO$_x$ emissions, a secondary air or dilution air is injected at 0.1 m from the fuel injector. The secondary air is injected in the combustion chamber though six side air inlets each with a diameter of 16 mm (Fig. 2) with an injection velocity of 6 m/s, a temperature of 300 K, a turbulence intensity of 10%, and a mixture fraction $f = 0$. The can combustor outlet has a rectangular shape (Fig. 2) with an area of 0.0150 m^2 [3]. The mesh generated for the can combustor (Fig. 2) consists of 106,651 cells or elements (74,189 tetrahedra, 30,489 wedges and 1,989 pyramids).

Table 2 shows the composition and lower heating values of the five fuels selected in this study for the CFD analysis. The range of the constituents volume fractions for the selected fuels are: methane (CH_4) = 45%-95%, carbon dioxide (CO_2) = 0-40%, and nitrogen (N_2) = 0-15%. The carbon dioxide to methane ratio for the five gases is between 0 and 0.89 (zero for the natural gas and 0.89 for the landfill biogas). Table 2 shows also that, the lower heating values for the biogas fuels are smaller compared to the lower heating value of natural gas. The biogas landfill is the low grade bio gas fuel with only 12.3 MJ/kg heating value compared to 50 MJ/kg for natural gas.

4. Results and Discussion

The results of the combustion performance and emissions of conventional fuel (natural gas) and alternative fuel (biogas) in gas turbine can combustor are presented in this paper.

Figs. 3 and 4 show the contours of the predicted gas temperature in the x-y and z-x planes for the steady state combustion of natural gas, biogas, and natural gas/biogas mixtures in gas turbine can combustor. The results show a maximum gas temperature for methane fuel combustion of 2,110 K. The maximum predicted temperature for the methane fuel combustion compares well with the theoretical adiabatic flame temperature (2,200 K). The static temperature contours show a peak gas temperature in the primary reaction zone. The fuel injected from the six injectors is mixed first with the swirling air before burning in the primary reaction zone. The gas temperature decreases after the primary reaction zone due to the dilution of the flame with secondary air flow. The flame structure and the temperature in the reaction zone are affected by the turbulent air flow (flame/flow interaction). Highly turbulent air flow and the air flow turbulent characteristics (characteristic length and time scales, velocity fluctuations, and re-circulations zones) will affect the turbulent burning velocity of the flame, the flame structure, and the burning rates (rate

of conversion of reactants to products in kg/s). The velocity vectors in the z-x plane and the recirculation zones in the primary reaction zone are shown in Fig. 5. The primary air is accelerated in the z direction from an initial velocity of 10-20 m/s at the entrance of the combustors due to the presence of swirls vanes [3]. The re-circulation regions produced near the fuel injection region help to mix the fuel and air. In the primary reaction zone, a good air fuel mixing is obtained (Fig. 5). The gas fuel is burned efficiently and the gas emissions at the exit from the can combustor are reduced. The contours (in the x-y plane) of the velocity swirling strength are shown in Fig. 6. The contours in Fig. 6 show recirculation zones near the fuel injection regions (near the primary reaction zone) with strong swirling strength. Higher combustion efficiency is obtained in the regions with strong swirling strength. The velocity swirling strength decreases downstream with the increase of the axial distance Z.

The effects of fuel compositions and lower heating values on static temperatures contours and the static temperature profiles inside the can combustors are shown in Figs. 3, 4 and 7. The results show that, the gas temperature inside the can combustor decreases by reducing the amount of methane and increasing the concentrations of carbon dioxide. The dilution of hydrocarbon fuel (CH_4) with carbon dioxide (CO_2) and nitrogen (N_2) reduce the flame temperature. It is noted that, the nitrogen and carbon dioxide ($N_2 + CO_2$) in the fuel is 2% for natural gas, 35% for biogas produced from anaerobic digester and 55% for biogas from landfill). The inert gas such as CO_2 and nitrogen absorb the heat from the combustion process and act as flame inhibitors. The presence of carbon dioxide and nitrogen reduces the burning velocity [12] of the flame and the burning rate (rate of conversion of reactants to combustion products).

Biogas air mixtures combustion produced lower gas temperature inside the combustor compared to natural gas fuel. The gas temperature for biogas fuel

(a) NG
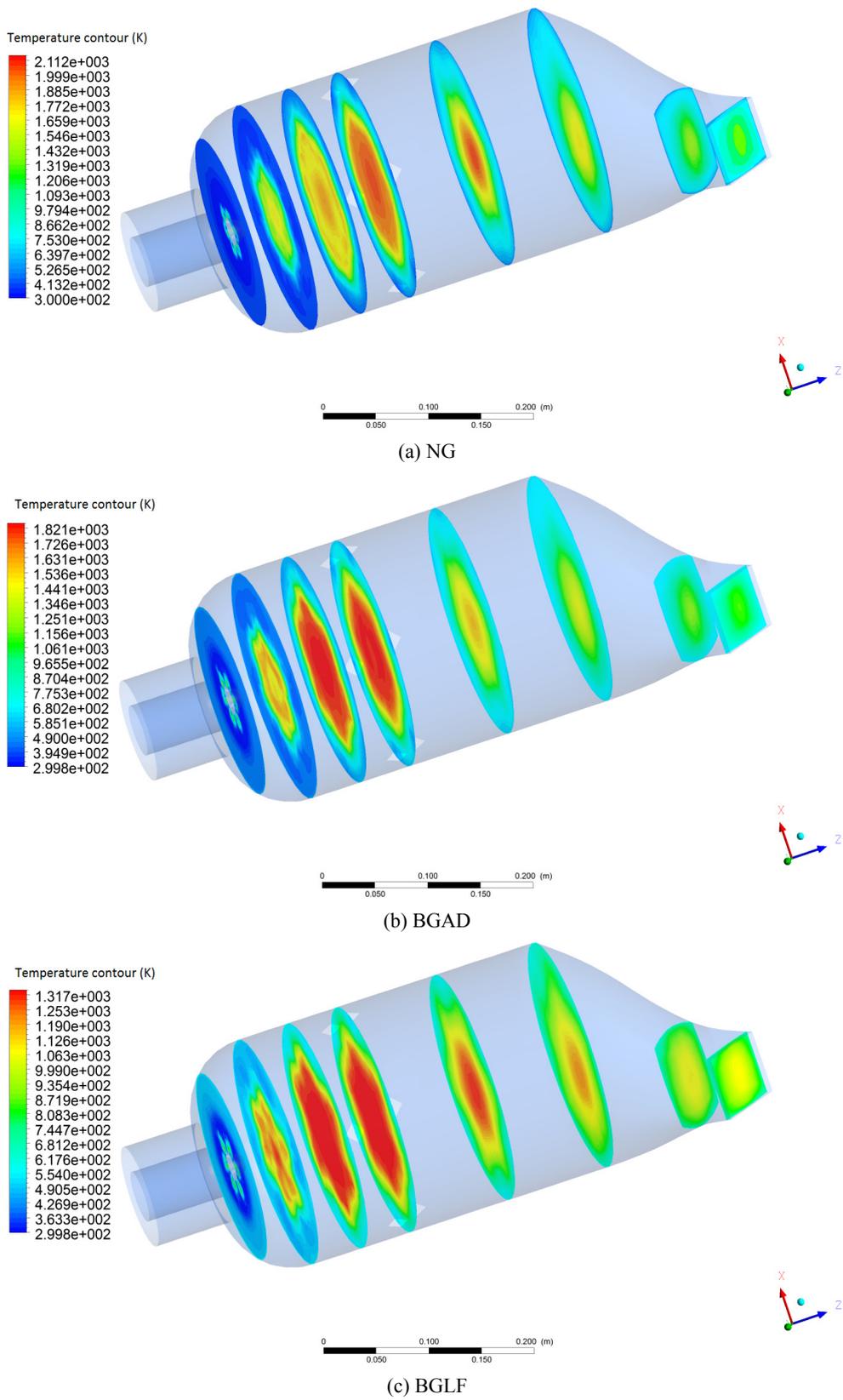
(b) BGAD

(c) BGLF

Fig. 3   Static temperature contours in the x-y plane: (a) NG, (b) BGAD and (c) BGLF.
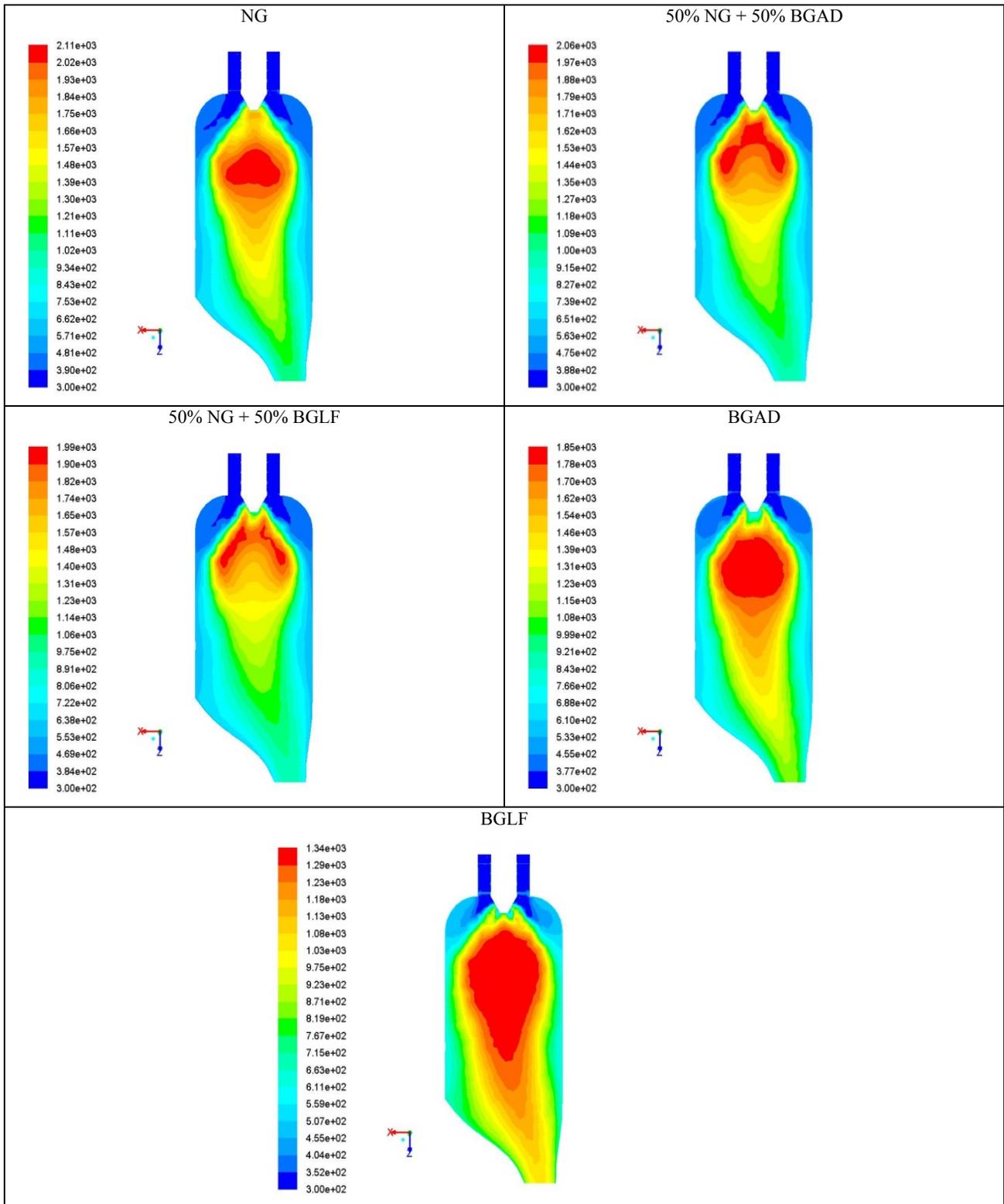
**Fig. 4   Contours of static temperature (K) in the z-x plane.**
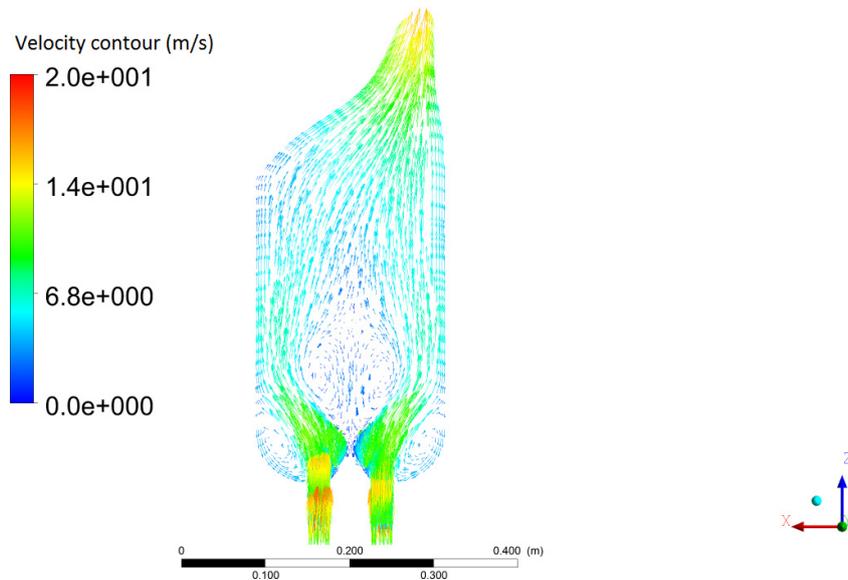
**Fig. 5　Velocity vectors in the z-x plane.**
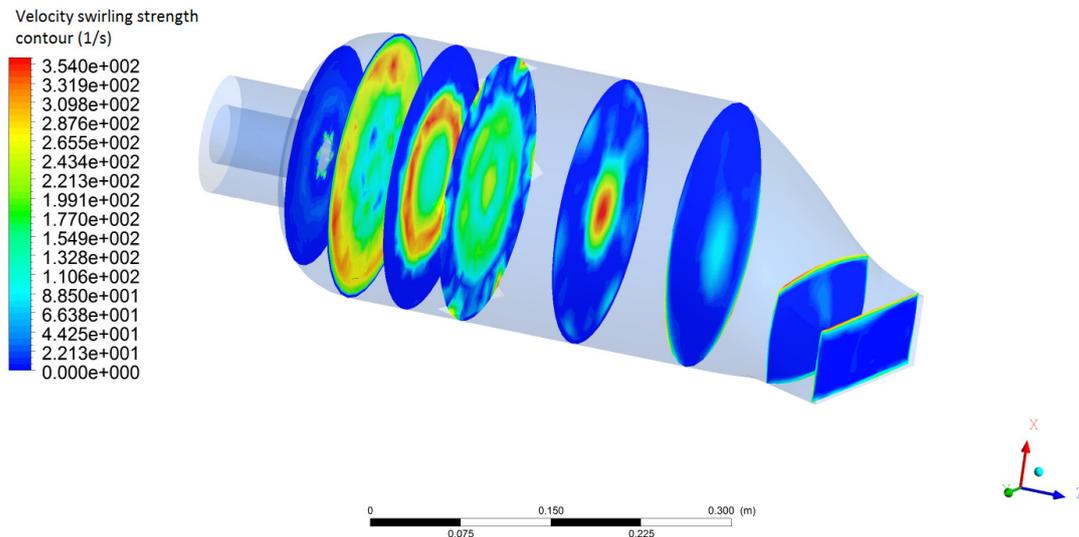
Fig. 6　Velocity swirling strength in the x-y plane.

combustion depends on the carbon dioxide to methane ratio (CO_2/CH_4) as shown in Table 3. The peak gas temperature decreases as the CO_2/CH_4 ratio increases. The peak gas temperature decreases by 37% and 22%, respectively for the biogas-landfill ($CO_2/CH_4 = 0.89$) and biogas anaerobic digester ($CO_2/CH_4 = 0.54$) compared to natural gas fuel.

The NO_x emissions from natural and biogas fuels combustion were also calculated in this study. The centerline NO_x (ppm) emissions inside the can combustor are shown in Fig. 8. The results show that,

the NO_x emissions inside the combustor decreases when the baseline fuel (natural gas) is replaced with biogas fuel with lower heating value. The thermal NO_x emission is function of the gas temperature. High gas temperature inside the can combustor will produce high NO_x (mainly NO) emissions. The presence of non-combustible constituents in the biogas such as carbon dioxides and nitrogen reduces the temperature of the flame and consequently the NO mass fractions. This reduction is proportional to the amount of inert constituents in biogas fuel.
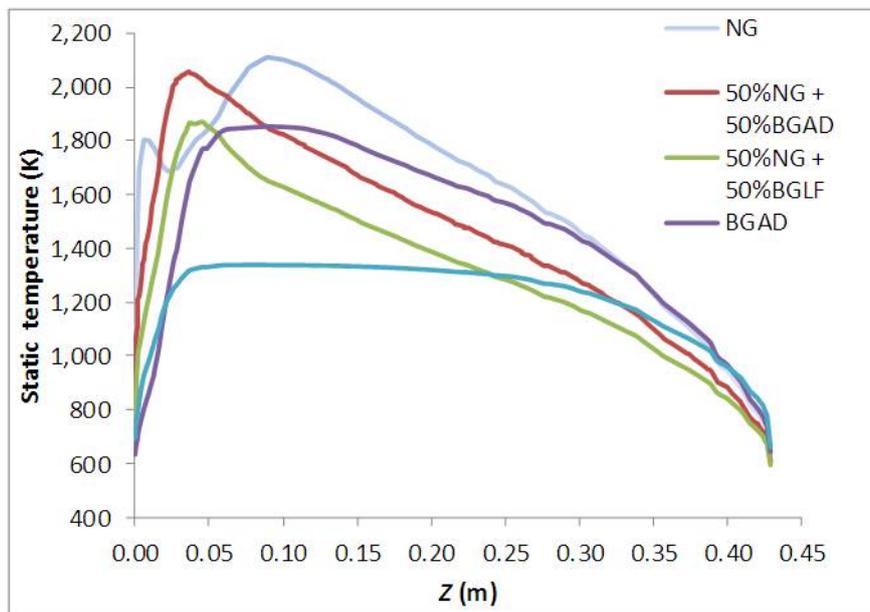
Fig. 7   Centerline (x = 0, y = 0) static temperature profiles.

Table 3   Effect of carbon dioxide to methane ratio on static temperature, CO and CO_2 mole fractions inside the combustor.

	NG	Mixture 50% NG 50% BGAD	Mixture 50% NG 50% BGLF	BGAD	BGLF
CO_2/CH_4	0	0.22	0.29	0.54	0.89
Peak flame temperature (K)	2,109	2,054	1,866	1,852	1,337
Peak CO mole fractions	9.85×10^{-2}	3.92×10^{-2}	4.38×10^{-3}	2.22×10^{-4}	1.32×10^{-7}
Peak CO_2 mole fractions	9.38×10^{-2}	17.5×10^{-2}	20×10^{-2}	35×10^{-2}	40×10^{-2}
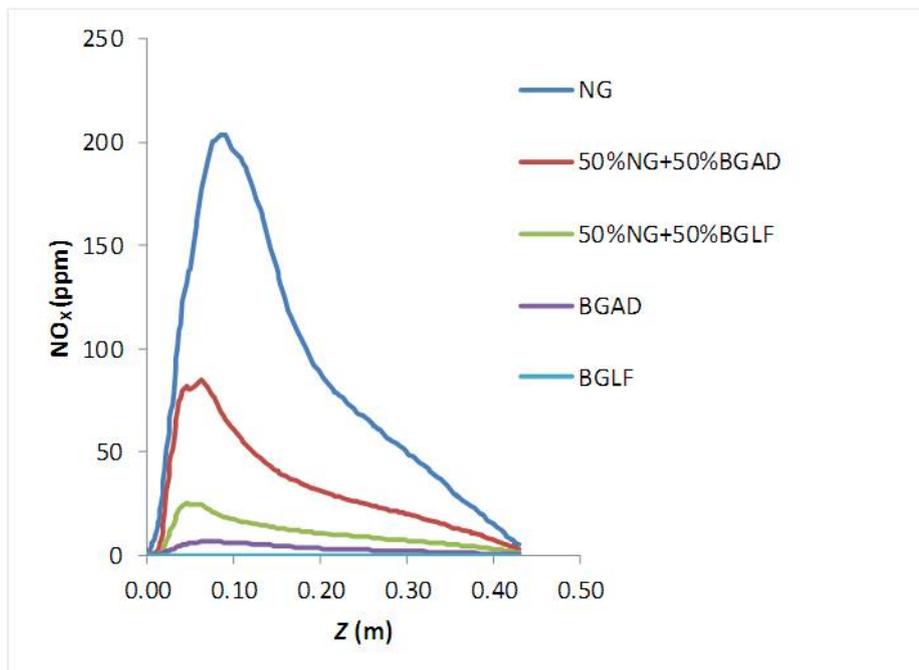
Fig. 8   Centerline NO_x emissions profiles.

Table 4   Effect of carbon dioxide to methane ratio on the temperature and species mole fractions at the exit of the combustor.

	NG	Mixture 50% NG 50% BGAD	Mixture 50% NG 50% BGLF	BGAD	BGLF
CO_2/CH_4	0	0.22	0.29	0.54	0.89
Exit average gas Temperature (K)	869	818	786	889	879
Exit average CO_2 mole fractions	2.2×10^{-2}	2.41×10^{-2}	2.37×10^{-2}	3.51×10^{-2}	4.2×10^{-2}
Exit average NO_x mole fractions	1.13×10^{-5}	5.68×10^{-6}	2.33×10^{-6}	0.40×10^{-6}	1.06×10^{-10}

The effect of biogas CO_2/CH_4 ratio on the peak flame temperature, CO and CO_2 emissions inside the can combustor (3D geometry) is summarized in Table 3. An increase of the CO_2/CH_4 ratio for the biogas fuel result in a decrease of the peak flame temperature and CO mole fractions and an increase of the CO_2 mole fractions inside the can combustor. The effect of the biogas CO_2/CH_4 ratio on the combustion and emissions characteristics at the exit of the can combustor was also determined in this study. The average flame temperature, CO_2 mole fractions and NO_x mole fractions at the exit of the combustor are presented in Table 4. The NO_x emissions at the exit of the combustor decrease with the increase of the biogas CO_2/CH_4 ratio but the emissions of CO_2 at the exit of the combustor increase with an increase of CO_2 fractions in the biogas fuels (higher CO_2 input).

5. Conclusions

Three dimensional CFD analyses of natural gas, biogas anaerobic digester, biogas landfill and natural gas/biogas fuels combustion in gas turbine can combustor are presented in this study. The effect of the biogas fuel composition, and fuel heating values on flame shape, flame temperature, carbon dioxide (CO_2), carbon monoxide (CO) and nitrogen oxides (NO_x) emissions was determined in this study. The results show lower flame temperatures for the biogas and biogas/natural gas mixtures compared to the adiabatic flame temperature of natural gas. The flame temperature for biogas fuel combustion depends on the carbon dioxide to methane ratio (CO_2/CH_4). The peak flame temperature decreases by 37% and 22%,

respectively for the biogas-landfill (CO_2/CH_4 = 0.89) and biogas anaerobic digester (CO_2/CH_4 = 0.54) compared to natural gas fuel. The presence of inert gas (CO_2) with methane cools down the reaction by absorbing energy from the combustion and modifies the reaction zone by reducing the burning velocity of the flame and the burning rate. The reaction zone is elongated when large amount of CO_2 is added to methane. The emissions from biogas combustion vary with the composition of biogas. The higher CO_2 percentage in the biogas fuel, the lower is the NO_x emissions and the higher is the CO_2 emissions at the exit of the combustor. The CO emissions also decrease by increasing the CO_2/CH_4 ratio of the biogas fuel.

References

[1]   Ghenai, C. 2014. "Energy-Water-Carbon Interconnection: Challenges and Sustainable Solution Methods and Strategies." *International Journal of Thermal & Environmental Engineering* 7 (2): 57-64.

[2]   Lieuwen, T., McDonell, V., Santavicca, D., and Sattelmayer, T. 2008. "Burner Development and Operability Issues Associated with Steady Flowing Syngas Fired Combustors." *Combustion Science and Technology* 180 (6): 1167-90.

[3]   Ghenai, C. 2010. "Combustion of Syngas Fuel in Gas Turbine Can Combustor." *Advances in Mechanical Engineering* 2 (January): 13.

[4]   Brdar, R. D., and Jones, R. M. 2000. "GE IGCC Technology and Experience with Advanced Gas Turbines." GE Power Systems, GER-4207.

[5]   Kwiatkowki, K., Dudynski, M., and Bajer, K. 2013. "Combustion of Low Waste Biomass Syngas." *Flow Turbulence Combust* 91 (4): 749-72.

[6]   Oluyede, E. O. 2006. *Fundamental Impact of Firing Syngas in Gas Turbines, Gas Turbine Industrial*

Fellowship Program. Project report.

[7] Giles, D. E., Som, S., and Aggarwal, S. K. 2006. "NO$_x$ Emission Characteristics of Counterflow Syngas Diffusion Flames with Airstream Dilution." *Fuel* 85 (12-13): 1729-42.

[8] Zbeeb, K., and Ghenai, C. 2013. "Syngas Fuel Combustion in Re-circulating Vortex Combustor." *Journal of Energy and Power Engineering* 7 (10): 1852-64.

[9] Alavandi, S. K., and Agarwal, A. K. 2008. "Experimental Study of Combustion of Hydrogen-Syngas/Methane Fuel Mixtures in a Porous Burner." *International Journal of Hydrogen Energy* 33 (4): 1407-15.

[10] Schefer, R. W. 2001. "Combustion of Hydrogen Enriched Methane in a Lean Premixed Swirl Burner." Presented at the 2001 DOE (Department of Energy) Hydrogen Program Review, Baltimore, Maryland.

[11] Rahm, S., Goldmeer, J., Moilere, M., and Eranki, A. 2009. "Addressing Gas Turbine Fuel Flexibility." Presented at the Power-Gen Middle East Conference, Manama, Bahrain.

[12] Razbani, O., Mirzamohammad, N., and Assadi, M. 2011. "Literature Review and Road Map for Using Biogas in Internal Combustion Engines." Presented at the 3rd Internal Conference on Applied Energy, Perugia, Italy.

[13] Anggono, W., Wardana, I., Lawes, K., Hughes, K. J., Wahyudi, S., and Hamidi, N. 2012. "Laminar Burning Characteristics of Biogas-Air Mixtures in Spark Ignited Premix Combustion." *Journal of Applied Sciences Research* 8 (8): 4126-32.

[14] Barik, D., Sah, S., and Murugan, S. 2013. "Biogas Production and Storage for Fueling Internal Combustion Engines." *International Journal of Emerging Technology and Advanced Engineering* 3 (3): 193-202.

[15] Colorado, A. F., Herrera, B. F, and Amell, A. A. 2010. "Performance of Flameless Combustion Furnace Using Biogas and Natural Gas." *Bioresource Technology* 101 (7): 2443-9.

[16] Cheng, P. 1964. "Two-Dimensional Radiating Gas Flow by a Moment Method." *AIAA Journal* 2 (9):1662-4.

[17] Siegel, R., and Howell, J. R. 1992. *Thermal Radiation Heat Transfer.* Washington, DC: Hemisphere Publishing Corporation.